Korean J. Chem. Eng., **15**(1), 64-70 (1998)

SYNTHESIS AND CYCLING BEHAVIOR OF $LiMn_2O_4$ CATHODE MATERIALS PREPARED BY GLYCINE-ASSISTED SOL-GEL METHOD FOR LITHIUM SECONDARY BATTERIES

Yang-Kook Sun†, Dong-Won Kim, Sung-Ho Jin, Yoo-Eup Hyung*, Sung-In Moon* and Dong-Kyu Park**

Polymer Materials Laboratory, Chemical Sector, Samsung Advanced Institute of Technology, 103-12, Moonji-dong, Yusong-Gu, Taejon 305-380, Korea
*Korea Electrotechnology Research Institute, P.O.BOX 20, Changwon 641-600, Korea
**Dept. of Chemistry, Kyungsung University, 110 Daeyeon-Dong, Nam-Ku, Pusan 608-736, Korea
(Received 13 August 1997 • accepted 15 November 1997)

Abstract – Spinel-type $LiMn_2O_4$ powders having submicron, narrow particle-size distribution and excellent phase-pure particles have been synthesized at low temperatures from metal acetate aqueous solution containing glycine as a chelating agent by a sol-gel method. The dependence of the physicochemical properties and cycling characteristics of the spinel $LiMn_2O_4$ powders on the various calcination temperatures has been extensively studied. It was found that the physicochemical properties of the $LiMn_2O_4$ powders could be controlled by simply varying the calcination temperature. Glycine-assisted $LiMn_2O_4$ powders have shown excellent rechargeability and delivered discharge capacity of 119 mAh/g for more than 150th cycles in Li/polymer electrolyte/$LiMn_2O_4$ cells.

Key words: Lithium Secondary Battery, Lithium Manganese Oxide, Sol-Gel Method, Chelating Agent, Glycine

INTRODUCTION

Spinel-type $LiMn_2O_4$ has been extensively studied for the most promising cathode materials for lithium secondary batteries with high energy density [Feng et al., 1996; Xia et al., 1997]. This material offers several advantages; it is easier to prepare, cheaper and less toxic than layered oxides such as $LiCoO_2$ and $LiNiO_2$ [Pistoia et al., 1993; Macklin et al., 1991; Momchilov et al., 1993; Guyomard et al., 1994]. For commercial applications, it is important to produce $LiMn_2O_4$ powders with excellent cyclability and capacity retention at relatively high current densities. However, there is a problem in that its capacity fading and cyclability in the 4 V region are inferior to those of layered oxides. The reason for capacity fading has not been clearly established, but some possible factors have been proposed [Gummow et al., 1994; Jang et al., 1996]: (1) an instability of the electrolyte at the charged state, (2) a slow dissolution of the $LiMn_2O_4$ electrode to the disproportion reaction ($2Mn^{+3} \rightarrow Mn^{+4} + Mn^{+2}$), (3) a phase transition from cubic to tetragonal symmetry due to Jahn-Teller distortion in a deeply discharged state. In order to improve capacity fading and cyclability of the $LiMn_2O_4$ powders in the 4 V region, the effect of adding excess lithium to the stoichiometric $LiMn_2O_4$ spinel [Guyomard et al., 1994], manganese-substituted stoichiometric $LiMn_2O_4$ spinel [Gummow et al., 1994; Tarascon et al., 1991; Guohua et al., 1996] and the change of synthesis atmosphere [Richard et al., 1994] have been studied.

†To whom all correspondence should be addressed.
E-mail: yksun@saitgw.sait.samsung.co.kr

The performance of $LiMn_2O_4$ powders used for lithium secondary batteries strongly depends on its synthetic method [Gao et al., 1996]. Usually, the preparation of $LiMn_2O_4$ powders is done by solid-state reaction which consists of extensive mechanical mixing of lithium hydroxide, carbonate, or nitrate with manganese oxide, hydroxide, or carbonate followed by high temperature calcination and extended grinding. This method, however, has several disadvantages: inhomogeneity, irregular morphology, larger particle size with broader particle size distribution, poor control of stoichiometry, higher temperatures and longer periods of calcination.

There have been a few reports on the synthesis of cathode active materials for lithium secondary batteries by using a solution method [Liu et al., 1996; Cho et al., 1997; Qiu et al., 1997]. Among the solution methods, a sol-gel method can produce highly homogeneous powders having submicron-sized particles with narrow particle-size distribution and thus enhanced performance of electrodes [Liu et al., 1996]. In spite of these advantages, there have been few reports on preparing $LiMn_2O_4$ powders by a sol-gel method [Barboux et al., 1991; Tsumura et al., 1993; Prabaharan et al., 1995; Liu et al., 1996]. Recently, the authors have reported that ultrafine $LiCoO_2$ powders with an average particle size of 30-50 nm, highly homogeneous $LiCoO_2$ powders with an average particle size of 30-60 nm, and highly crystalline $LiNiO_2$ powders having submicron, narrow particle-size distribution, could be successfully synthesized through the sol-gel method using PAA, malic acid, and PVB as chelating agent, respectively [Sun et al., 1996, 1997; Oh et al., 1997]. It is well known that the physicochemical properties of oxide powders strongly depend on the chelating agent used in the sol-gel method [Teraoka

et al., 1991].

In this study, $LiMn_2O_4$ powders with uniform submicron-sized particles were synthesized by a sol-gel method using glycine as a chelating agent at considerably lower temperatures and shorter time. The effect of calcination temperatures on the physicochemical properties and cycling characteristics of $LiMn_2O_4$ powders in Li/1 M $LiBF_4$-EC/DEC/$LiMn_2O_4$ cells and Li/polymer electrolyte/$LiMn_2O_4$ cells was extensively investigated.

EXPERIMENTAL

$LiMn_2O_4$ powders were prepared according to the following procedure. A stoichiometric amount of lithium acetate and manganese acetate (Acros Co., high purity) salts with the cationic ratio of Li : Mn=1 : 2 was dissolved in distilled water and mixed completely with an aqueous solution of glycine (Aldrich Chemical Co.). A molar ratio of glycine to total metal ions of unity was used to make a gel. Ammonium hydroxide and nitric acid were slowly added to this solution with constant stirring for 5 hrs until a pH of 4-7.5 was achieved. The resultant solution was evaporated at 70-80 °C for 5 hrs until a transparent sol was obtained. To remove water in the sol, the transparent sol was heated at 70-80 °C while being mechanically stirred with a magnetic stirrer. As the water evaporated, the sol turned into a viscous transparent gel. The gel precursors obtained were decomposed at 300-800 °C for 24 hrs in air to obtain phase-pure polycrystalline $LiMn_2O_4$ powders.

The thermal decomposition behavior of the gel precursor was examined by means of thermogravimetry (TG, DuPont, TA2050) and differential thermal analysis (DTA, DuPont, TA-2050). Powder X-ray diffraction (Rint-2000, Rigaku) using Cu-Kα radiation was used to identify the crystalline phase of the materials calcined at various temperatures. Rietveld refinement was then performed on the X-ray diffraction data to obtain the lattice constant. The morphological changes of the particles were observed with a field emission scanning electron microscope (S-4100, Hitachi Co.). The specific surface area was determined by the BET method (ASAP2100, Micrometrics) by nitrogen adsorption.

Poly(acrylonitrile-co-methyl methacrylate-co-styrene) terpolymer was synthesized via emulsion polymerization with monomer reactants of acrylonitrile (AN), methyl methacrylate (MMA) and styrene (ST) in distilled water at 60 °C [Kim et al., 1997]. Potassium persulfate ($K_2S_2O_8$) was used as a free-radical water-soluble initiator, and sodium lauryl sulfate was used as an emulsifier. The copolymerization was continued for 5 hrs with vigorous agitation. The polymer was isolated by filtration and washed successively with distilled water at 80 °C to remove any impurities such as residual monomer and initiator. The product was then dried in a vacuum oven at 100 °C for 24 hrs. A white powder was obtained as a product. The molar composition of AN : MMA : ST in the terpolymer synthesized was determined to be 54 : 32 : 14 by ^1H NMR spectroscopy. For brevity, the P(AN-co-MMA-co-ST) terpolymer synthesized will be designated as AMS in this paper.

The electrochemical properties of $LiMn_2O_4$ powders were determined by three-electrode method in Li/(liquid electrolyte)/$LiMn_2O_4$ cells and two electrode method in Li/(polymer electrolyte)/$LiMn_2O_4$ cells. A three-electrode electrochemical cell was used for the galvanostatic charge-discharge experiments. The reference and counter electrodes were constructed from lithium foil (Cyprus Co., 99.999 %). The electrolyte used was a 1 : 1 mixture of ethylene carbonate (EC) and diethyl carbonate (DEC) containing 1 M $LiBF_4$ (Mitsubishi Co., 99.99 %). The cathode was a mixture of 73 wt% active material, 20 wt% Ketzenblack EC, 7 wt% Teflon binder. The mixture were then dispersed in isopropyl alcohol and spread on Exmet, followed by pressing and drying at 120 °C for 3 hrs. The cells were assembled in an argon-filled dry box. Charge-discharge cycling was performed galvanostatically at a current density of 1 mA/cm^2, with a cut-off voltage of 3.6 to 4.3 V (vs. Li/Li^+).

The polymer electrolyte was made from AMS terpolymer, plasticized by a solution of $LiClO_4$ in a 1 : 1 mixture of ethylene carbonate (EC) and propylene carbonate (PC). Typical polymer electrolyte compositions were AMS terpolymer 10 wt%, EC 40 wt%, PC 37 wt%, $LiClO_4$ 7 wt%, and SiO_2 7 wt%. The ionic conductivity of free-standing polymer electrolyte was 1.8×10^{-3} $\Omega^{-1}cm^{-1}$ at room temperature. The composite cathode was prepared by mixing the as-synthesized $LiMn_2O_4$ powders, super P, and the polymer electrolyte in a weight ratio of 59.5 : 31.2 : 9.3 and then coating the resultant paste on an Al foil current collector. The anode consisted of 50 μm thick Li foil (Cyprus Foote Mineral Co.) pressed onto a Cu foil current collector. The polymer electrolyte sandwiched between the two electrodes was sealed in a metallized plastic bag. Charge-discharge cycling was performed galvanostatically at a current density of 0.1 mA/cm^2, with a cut-off voltage of 3.0 to 4.3 V (vs. Li/Li^+).

RESULTS AND DISCUSSION

The transparent gel could be formed from the solution with initial pH of 4-9 in this study. The transparency and uniform color of the gel precursors indicate that its composition was homogeneous.

Fig. 1 shows the thermogravimetry (TG) and differential thermal analysis (DTA) of the gel precursor prepared by the molar ratio of glycine to total metal ions of 1.0. The weight loss of the gel precursor terminated at 400 °C, and three discrete weight loss regions occurred at 200-250 °C, 250-360 °C, and 360-400 °C. The weight loss in the temperature range of 200-250 °C corresponded to the combustion of glycine that occurred with an exothermic peak of the DTA curve at 250 °C. The weight loss in the temperature range of 250-360 °C was associated with the decomposition of acetate ions which was accompanied by an exothermic peak of the DTA curve at 280 °C. This argument was supported by the observation that the gel precursors turned into fluffy dark powders after being calcined at this stage. The weight loss in the temperature range of 360-400 °C was due to the combustion of the remaining organic constituents which occurred with larger exothermic peaks at 380 °C.

Fig. 2 shows the X-ray diffraction (XRD) patterns for the gel-derived materials calcined at various temperatures for 24 hrs in air, where the molar ratio of glycine to total metal

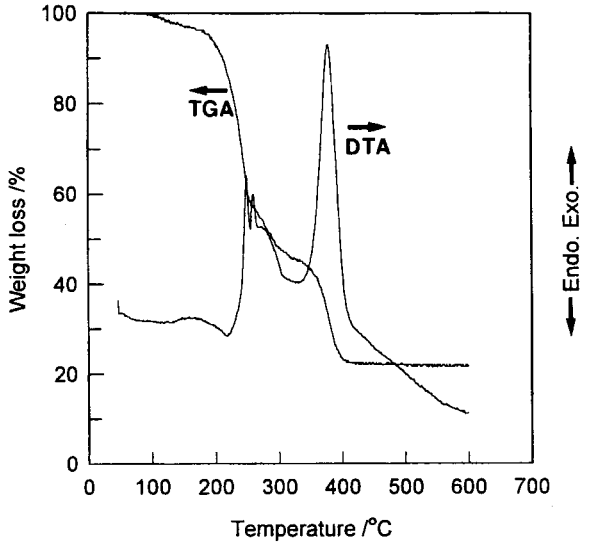

Fig. 1. Thermogravimetric and differential thermal analysis of the gel precursors pretreated in vacuum drying at 80 °C prior to thermal analysis at air flow rate of 40 cc/min. Heating rate was 5 °C/min.

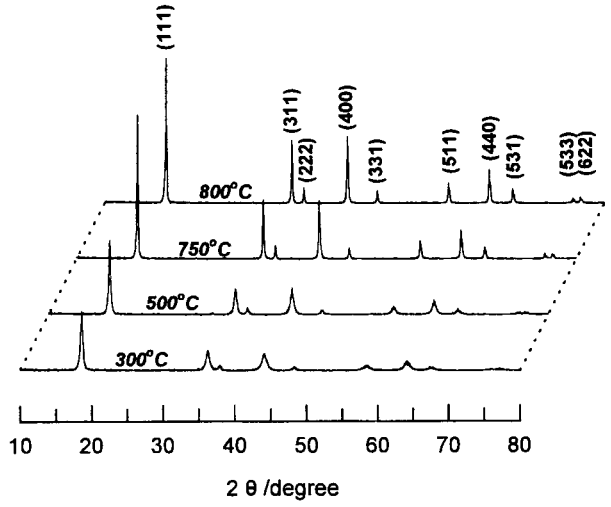

Fig. 2. X-ray diffraction patterns of gel-derived materials calcined at various temperatures. The molar ratio of glycine acid to total metal ions was 1.0.

ions was 1.0. The X-ray diffraction pattern for the material calcined at 300 °C represents the crystalline $LiMn_2O_4$ spinel beginning to appear. Impurity peaks, such as Li_2CO_3 and $MnCO_3$, are not observed; they are often found in other low temperature techniques. There is a gradual increase in the peak intensities accompanied by sharpening of the peaks with increasing calcination temperature, which indicates an increase of crystallinity. The crystalline $LiMn_2O_4$ phase has a cubic spinel structure with a space group Fd3m. When the calcination was performed above 750 °C, it is seen that the peaks were abruptly sharpened owing to the high bulk crystallization of the grains. The precursor was crystallized into a phase-pure $LiMn_2O_4$ spinel powder without any development of a minor phase throughout the calcination temperature range. This result strongly suggests that a sol-gel method requires much lower calcination temperature and shorter calcination time than a solid-state reaction, such as a calcination temperature of 650 to 750 °C and a time of 48 to 200 hrs of several intermittent cooling and grinding steps which are detrimental to the quality of the final products. This may be attributed to the fact that the materials derived from the gel precursors are of atomic scale and homogeneously mixed with each other, and thus have high sinterability. Similar results have already been reported where $LiCoO_2$, and $LiNiO_2$ powders were synthesized by the sol-gel method using various chelating agents such as PAA and malelic acid, and PVB, respectively [Sun et al., 1996, 1997; Oh et al., 1997].

Fig. 3 shows the dependence of the lattice constant a of the cubic unit cell of the same material as shown in Fig. 2 on the calcination temperature. The figure shows that the lattice constant a increases almost linearly from 8.1910 to 8.2304 Å with increasing calcination temperature from 300 °C to 800 °C, respectively. It is speculated that the value of the manganese average oxidation state in the spinel phase is closely related to the lattice constant a of the cubic unit cell. It is reported that the lattice constant of $Li_{1+x}Mn_{2-x}O_4$ powders should always be minimized at fixed composition to have fewer oxygen vacancies [Gao et al., 1996]. A lower calcination temperature results in a more oxidized manganese cation because manganese ions are stable preferentially as Mn^{4+} at lower temperatures [Masquelier et al., 1996]. The atomic radius of Mn^{4+} is smaller than that of Mn^{3+} and, thus the lattice constant a of the cubic unit cell for the materials calcined at higher temperature was larger than that of those calcined at lower temperature. Guyomard et al. have reported that the lattice constant a of slowly-cooled samples (c.a. 10 °C/hr) was significantly smaller and seldom exceeded about 8.23 Å in nominal formulations with x in $Li_xMn_2O_4$ greater than 1.0, which showed more stable maintenance of capacity [Guyomard et al., 1994].

Fig. 4 shows the dependence of specific surface area of

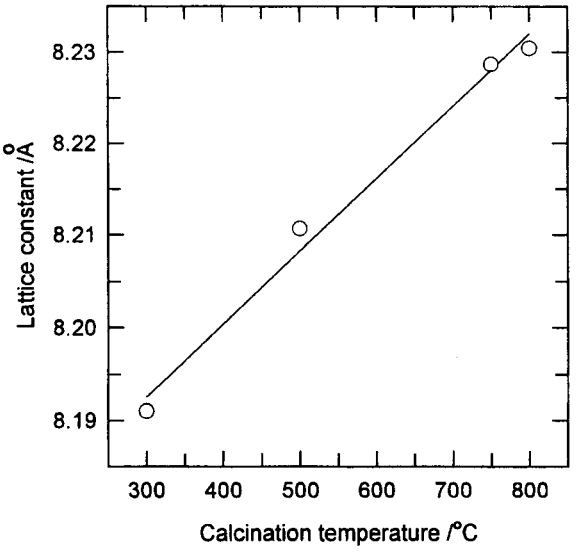

Fig. 3. Dependence of the lattice constant a of $LiMn_2O_4$ powders on the calcination temperature when the molar ratio of glycine acid to total metal ions was 1.0.

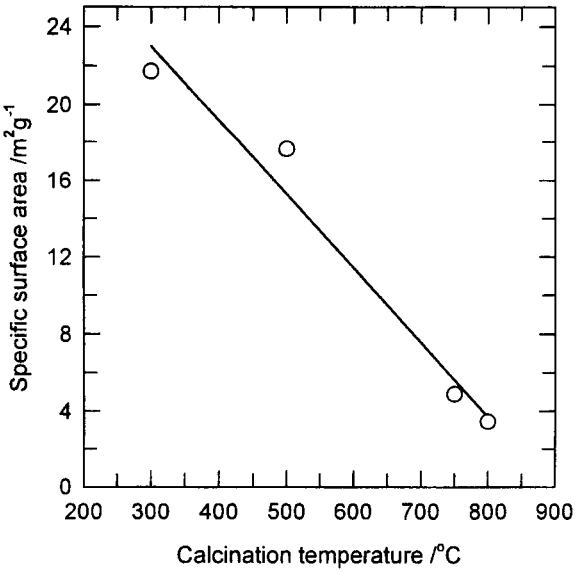

Fig. 4. Dependence of the specific surface area for $LiMn_2O_4$ powders on the calcination temperature when the molar ratio of glycine acid to total metal ions was 1.0.

the same material as shown in Fig. 3 on the calcination temperature. The specific surface area of the $LiMn_2O_4$ powders decreases linearly with increasing calcination temperature, due to the growth of $LiMn_2O_4$ crystallites. The specific surface area is 21.7 m^2/g and 3.4 m^2/g of the material calcined at 300 °C and 800 °C, respectively. Fig. 5 shows scanning electron micrographs (SEM) for the powders calcined the gel precursors of the molar ratio of glycine to total metal ions of 1.0 at various temperatures for 10 hrs in air. The presence of loosely agglomerated spherical particles with an average grain size of 60 nm was observed from the powders calcined at 300 °C. As calcination temperature was increased, growth kinetics were

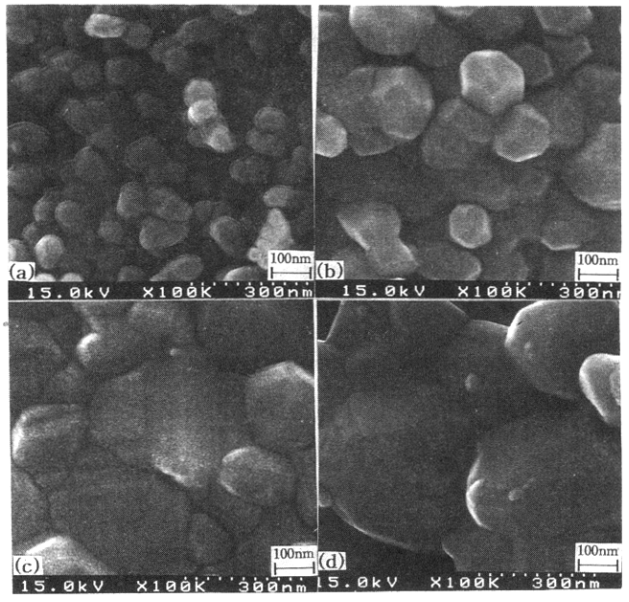

Fig. 5. Scanning electron micrographs of the $LiMn_2O_4$ powders calcined at (a) 300 °C, (b) 500 °C, (c) 750 °C, and (d) 800 °C.

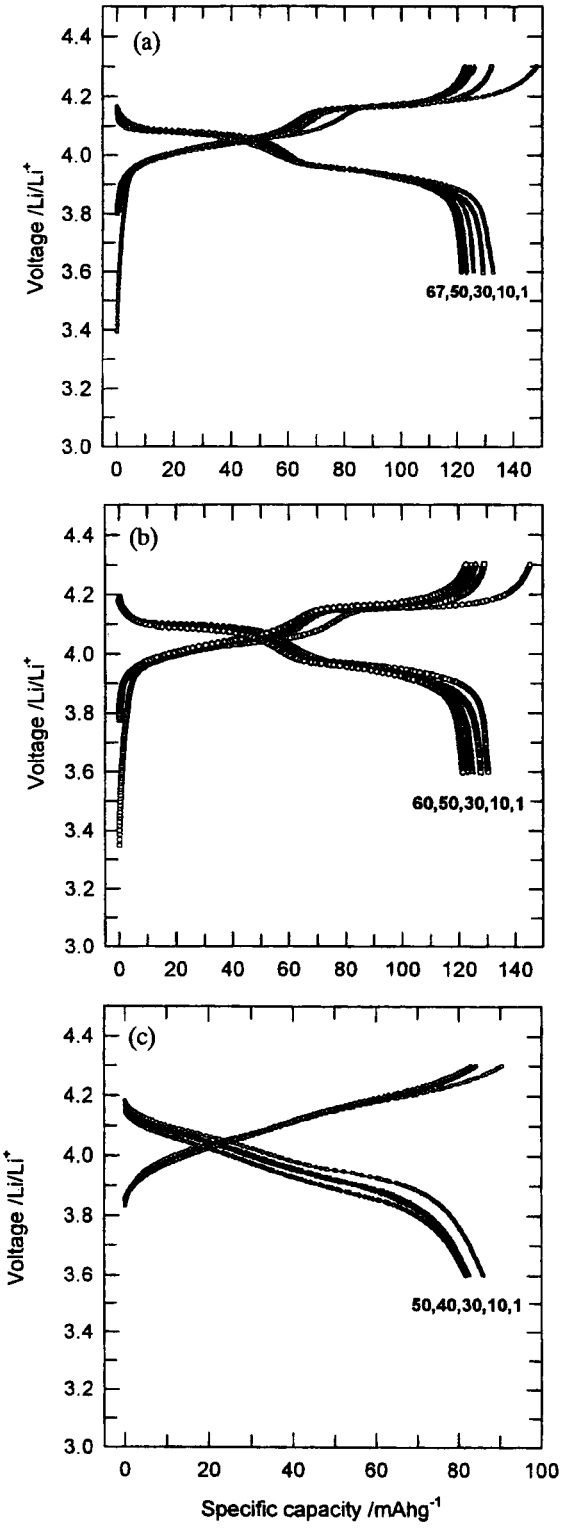

Fig. 6. Charge-discharge behavior with number of cycles for the Li/1 M $LiBF_4$-EC/DEC/$LiMn_2O_4$ cells at a constant charge/discharge current density of 1 $mAcm^{-2}$ using $LiMn_2O_4$ powders calcined at (a) 800 °C, (b) 750 °C, and (c) 300 °C.

favored and thus agglomerated spherical particles were changed to a larger particulate. When the gel precursors were heated at 500 °C, the particle size of the particulates increased to 100

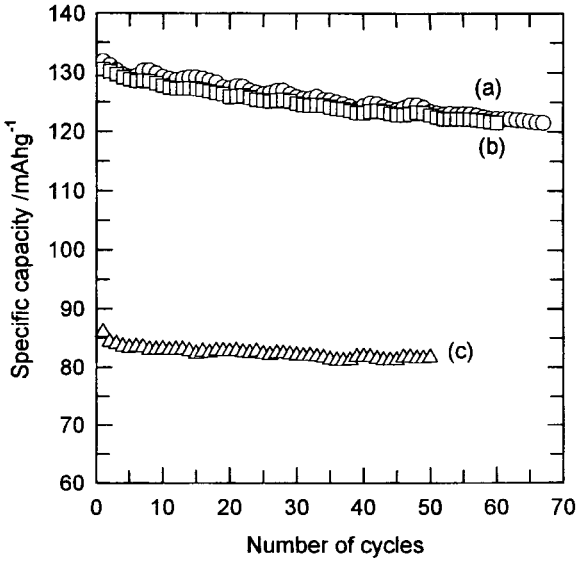

Fig. 7. Variation of specific discharge capacity with number of cycles for the Li/1 M $LiBF_4$-EC/DEC/$LiMn_2O_4$ cells using $LiMn_2O_4$ powders calcined at (a) 800 °C, (b) 750 °C, and (c) 300 °C. Cycling was carried out galvanostatically at constant charge/discharge current density of 1 mAcm^{-2} between 3.6 and 4.3 V.

nm with a fairly narrow particle-size distribution. For the materials calcined at 750 °C, it was observed that the particle size of the loosely agglomerated particulates abruptly increased to about 200 nm. When the materials were further calcined to 800 °C, the average particle size of the materials was 700 nm with narrow particle-size distribution.

From the above results, it was concluded that $LiMn_2O_4$ powders with a wide variety of physicochemical properties such as particle size, crystallinity, specific surface area, and microcrystallite morphologies could be controlled by simply varying the pyrolysis processing.

Fig. 6 and 7 show the charge-discharge behavior and the discharge capacities with number of cycles for the Li/1 M $LiBF_4$-EC/DEC/$LiMn_2O_4$ cells at a constant charge/discharge current density of 1 mAcm^{-2} using $LiMn_2O_4$ powders calcined at various temperatures, respectively. The Li/1 M $LiBF_4$-EC/DEC/$LiMn_2O_4$ cells using $LiMn_2O_4$ powders calcined at higher temperatures such as 800 and 750 °C [Fig. 6 (a) and (b)] showed that the charge/discharge curves have two distinct plateaus near 4.0 and 4.16 V_{Li/Li^+}. It was reported that each plateau delivered half of the total capacity, that the occurrence of the potential plateau near 4.0 V_{Li/Li^+} is due to the coexistence of two pseudo-phases of a lithium-diluted phase and a lithium-concentrated phase in a form of $Li_{0.5}Mn_2O_4$-$LiMn_2O_4$, and that the plateau near 4.16 V_{Li/Li^+} is due to the coexistence of λ-MnO_2-$Li_{0.5}Mn_2O_4$ [Pyun et al., in press]. On the contrary, the $LiMn_2O_4$ powders calcined at lower temperatures such as 300 °C [Fig. 6 (c)] showed that the charge-discharge curves have a slope in the potential range. The fact that no potential plateau was observed indicates that lithium-ion diffusion proceeds in a single phase of the low-crystalline electrode. The Li/1 M $LiBF_4$-EC/DEC/$LiMn_2O_4$ cells using $LiMn_2O_4$ powders calcined at 800, 750, and 300 °C (Fig. 7) initially

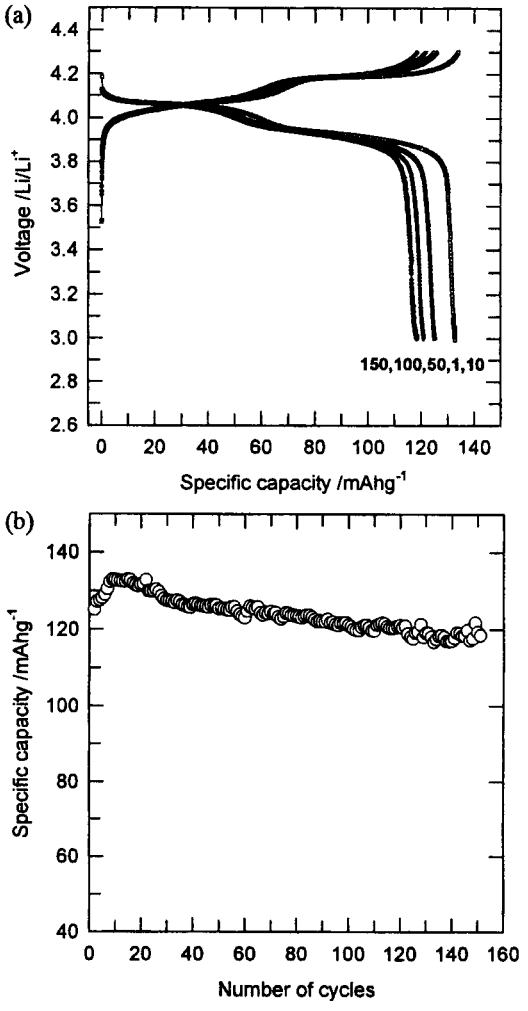

Fig. 8. (a) Cycling charge/discharge curves and (b) variation of specific discharge capacity with number of cycles for the Li/polymer electrolyte/$LiMn_2O_4$ cells using $LiMn_2O_4$ powders calcined at 800 °C. Cycling was carried out galvanostatically at constant charge-discharge current density of 0.1 mAcm^{-2} between 3.0 and 4.3 V.

delivered 133, 131, and 86 mAh/g, respectively. The capacity slowly decreased with cycling and remained at 122.4 mAh/g at the 67th cycle, 121.5 mAh/g at the 60th cycle, and 81.7 mAh/g at the 50th cycle for the $LiMn_2O_4$ powders calcined at 800, 750, and 300 °C, respectively. This shows very good capacity retention especially in view of the relatively high charge/discharge current density of 1 mAcm^{-2} or 0.5C. The capacity retention over the 67th, 60th, and 50th cycles is 92.2, 93.1, and 95 % of the initial discharge capacity for the $LiMn_2O_4$ powders calcined at 800, 750, and 300 °C, respectively. The poor crystallinity of $LiMn_2O_4$ powders calcined at lower temperatures is well consistent with the results of XRD patterns shown in Fig. 2 and the lattice constants a shown in Fig. 3. It is inferred from the above results that the $LiMn_2O_4$ powders calcined at higher temperatures have higher crystallinity and thus higher initial capacity but fast capacity fading due to Jahn-Teller distortion [Gummow et al., 1994; Jang et al., 1996]. Similar behavior was reported for $LiMn_2O_4$: fired to 300 °C, the initial capacity was 90 mAh/g with excellent cy-

cleability, while $LiMn_2O_4$ fired to 800 °C initially delivered 135 mAh/g and the capacity remained 127 mAh/g at the tenth cycle [Liu et al., 1996].

Fig. 8 shows the charge-discharge behavior and discharge capacities with number of cycles for the Li/(polymer electrolyte)/$LiMn_2O_4$ cells using $LiMn_2O_4$ powders calcined at 800 °C, where the molar ratio of glycine to metal ions was 1.0. The cells were activated by the first cycle and then were cycled between cut-off voltages of 3.0 and 4.3 V at a constant current density of 0.1 $mAcm^{-2}$ or 0.67C. The Li/(polymer electrolyte)/$LiMn_2O_4$ cells show that the discharge curves have two distinct plateaus, which means a well-defined spinel $LiMn_2O_4$ structure that is characteristic of the manganese-oxide spinel structure [Liu et al., 1996]. The Li/(polymer electrolyte)/$LiMn_2O_4$ cells initially delivered 125 mAh/g. The discharge capacity slowly increased with cycling and reached 133 mAh/g at the 9th cycle and then decreased with cycling and remained about 119 mAh/g up to the 150th cycle, which was 95 % of the initial capacity. It is well known that the interface resistance between polymer electrolyte/the composite $LiMn_2O_4$ might remain as small as possible and constantly remain to obtain good cyclability [Jiang et al., 1996]. Lithium ion intercalation is in general accompanied by molar volume change, and hence a mechanical stress field gradient across oxide electrode. The $LiMn_2O_4$ lattice change due to intercalation-induced stress is believed to deteriorate the electrical contact between the surfaces of the insertion-material particles and hence to decrease the capacity of the cathode during charge/discharge cycling [Jiang et al., 1996]. This phenomenon is severe to $LiMn_2O_4$ powders with broad particle size distribution. Therefore, it is inferred that excellent cyclability results from good contacts among the composite cathode interfaces ($LiMn_2O_4$/(polymer electrolyte)/carbon) due to a narrow particle-size distribution of our $LiMn_2O_4$ powders. The glycine-assisted sol-gel method is a very attractive method for synthesizing $LiMn_2O_4$-based cathode materials for lithium secondary batteries.

CONCLUSION

Spinel $LiMn_2O_4$ powders with submicron, monodispersed, and highly homogeneous particles were synthesized by a sol-gel method using an aqueous solution of metal acetate containing glycine as a chelating agent. The crystallinity and the lattice constant a of $LiMn_2O_4$ powders increased with increasing calcination temperature. Polycrystalline $LiMn_2O_4$ powders were found to be composed of very uniformly sized particulates with an average particle size of 60-700 nm and a specific surface area of 3.4-21.7 m^2/g. $LiMn_2O_4$ powders calcined at higher temperature have higher crystallinity and thus higher initial capacity but fast capacity fading. The glycine-assisted $LiMn_2O_4$ powders delivered initial capacity of 125 mAh/g and exhibited excellent cycling behavior (95 % of its initial capacity) in Li/polymer electrolyte/$LiMn_2O_4$ cells.

REFERENCES

Barboux, P., Tarascon, J. M. and Shokoohi, F. K., "The Use of Acetates as Precursors for the Low-Temperature Synthesis of $LiMn_2O_4$ and $LiCoO_2$ Intercalation Compounds", *J. of Solid State Chem.*, **94**, 185 (1991).

Cho, J., Guan, J. and Liu, M., "Electrochemical Properties of $LixMn_2O_4$ Composite Electrode in Cells Based on Glass-Polymer Composite Electrolytes", *Solid State Ionics*, **95**, 289 (1997).

Feng, L., Chang, Y., Wu, L. and Lu, T., "Electrochemical Behaviour of Spinel $LiMn_2O_4$ as Positive Electrode in Rechargeable Lithium Cells", *J. of Power Sources*, **63**, 149 (1996).

Gao, Y. and Dahn, J. R., "Synthesis and Characterization of $Li_{1+x}Mn_{2-x}O_4$ for Li-ion Batter Applications", *J. Electrochem. Soc.*, **143**, 100 (1996).

Gummow, R. J., Kock, A. de and Thackeray, M. M., "Improved Capacity Retention in Rechargeable 4 V Lithium/Lithium-Manganese Oxide (Spinel) Cells", *Solid State Ionics*, **69**, 59 (1994).

Guohua, Li, Ikuta, H., Uchida, T. and Wakihara, M., "The Spinel $LiM_yMn_{2-y}O_4$(M=Co, Cr, Ni) as the Cathode for Rechargeable Lithium Batteries", *J. Electrochem. Soc.*, **143**, 178 (1996).

Guyomard, D. and Tarascon, J. M., "The Carbon/$Li_{1+x}Mn_2O_4$ System", *Solid State Ionics*, **69**, 222 (1994).

Jang, D. H., Shin, Y. J. and Oh, S. M., "Dissolution of Spinel Oxides and Capacity Losses in 4 V $Li/Li_xMn_2O_4$ Cells", *J. Electrochem. Soc.*, **143**, 2204 (1996).

Jiang, Z. and Abraham, K. M., "Preparation and Electrochemical Characterization of Micron-Sized Spinel $LiMn_2O_4$", *J. Electrochem. Soc.*, **143**, 1591 (1996).

Kim, D.-W. and Sun, Y.-K., "Polymer Electrolytes Based on Acrylonitrile-Methyl Methacrylate-Styrene Terpolymer for Rechargeable Lithium Polymer Batteries", *J. Electrochem. Soc.*, submitted.

Liu, W., Farrington, G. C., Chaput, F. and Dunn, B., "Synthesis and Electrochemical Studies of Spinel Phase $LiMn_2O_4$ Cathode Materials Prepared by Pechini Process", *J. Electrochem. Soc.*, **143**, 879 (1996).

Liu, W., Kowal, K. and Farrington, G. C., "Electrochemical Characteristics of Spinel Phase $LiMn_2O_4$-Based Cathode Materials Prepared by the Pechini Process", *J. Electrochem. Soc.*, **143**, 3590 (1996).

Macklin, W. J., Neat, R. J. and Powell, R. J., "Performance of Lithium-manganese Oxide Spinel Electrodes in a Lithium Polymer Electrolyte Cell", *J. of Power Sources*, **34**, 39 (1991).

Masquelier, C., Tabuchi, M., Ado, K., Kanno, R., Kobayashi, Y., Maki, Y., Nakamura, O. and Goodenough, B., "Chemical and Magnetic Characterization of Spinel Materials in the $LiMn_2O_4$-$Li_2Mn_4O_9$-$Li_4Mn_5O_{12}$ System", *J. Solid State Chem.*, **123**, 255 (1996).

Momchilov, A., Manev, V., Nassalevska, A. and Kozawa, A., "Rechargeable Lithium Battery with Spinel-related MnO_2 II. Optimization of the $LiMn_2O_4$ Synthesis Conditions", *J. of Power Sources*, **41**, 305 (1993).

Oh, I.-H., Hong, S. A. and Sun, Y.-K., "Low-Temperature Preparation of Ultrafine $LiCoO_2$ Powders by the Sol-Gel Method", *J. Mater. Sci.*, **32**, 3177 (1997).

Pistoia, G. and Wang, G., "Aspects of the Li^+ Insertion into $Li_xMn_2O_4$ for 0<x<1", *Solid State Ionics,* **66**, 135 (1993).

Prabaharan, S., Michael, M. S., Kumar, T. P., Mani, A., Athinarayanaswamy, K. and Gangadharan, R., "Bulk Synthesis of Submicrometre Powders of $LiMn_2O_4$ for Secondary Lithium Batteries", *J. Mater. Chem.,* **5**, 1035 (1995).

Pyun, S.-I., Jeong, I.-J. and Choi, Y.-M., "The Effect of Lithium Content on the Electrochemical Lithium Intercalation into Amorphous and Crystalline Powdered $LiMn_2O_4$ Electrodes Prepared by Sol-Gel Method", *J. Power Sources,* In Press.

Qiu, X., Sun, X., Shen, W. and Chen, N., "Spinel $Li_{1+x}Mn_2O_4$ Synthesized by Coprecipitation as Cathodes for Lithium-Ion Batteries", *Solid State Ionics,* **93**, 335 (1997).

Richard, M. N., Fuller, E. W. and Dahn, J. R., "The Effect of Am- monia on the Spinel Electode Materials, $LiMn_2O_4$ and $Li(Li_{1/3}Mn_{5/3})O_4$", *Solid State Ionics,* **73**, 81 (1994).

Sun, Y.-K. and Oh, I.-H., "Synthesis of $LiNiO_2$ Powders by a Sol-Gel Method", *J. Mater. Sci. Lett.,* **16**(1), 30 (1997).

Sun, Y.-K. and Oh, I.-H., "Synthesis of Ultrafine $LiCoO_2$ Powders by the Sol-Gel Method", *J. Mater. Sci.,* **31**, 3617 (1996).

Tarascon, J. M., Wang, E., Shokoohi, F. K., McKinnon, W. R. and Colson, S., "The Spinel Phase of $LiMn_2O_4$ as a Cathode in Secondary Lithium Cells", *J. Electrochem. Soc.,* **138**, 2859 (1991).

Teraoka, Y., Kakebayashi, H., Moriguchi, I. and Kagawa, S., "Hydroxy Acid-Aided Synthesis of Perovskite-Type Oxides of Cobalt and Manganese", *Chem. Lett.*, 673 (1991).

Tsumura, T., Shimizu, A. and Inagaki, M., "Synthesis of $LiMn_2O_4$ Spinel via Tartates", *J. Mater. Chem.,* **3**, 995 (1993).

Xia, Y., Zhou, Y. and Yoshio, M., "Capacity Fading on Cycling of 4 V $Li/LiMn_2O_4$ Cells", *J. Electrochem. Soc.,* **144**, 2593 (1997).